

A Data Visualization Approach for Intersection Analysis using AIS Data

Ricardo Cardoso Pereira, Pedro Henriques Abreu, Evgheni Polisciuc and Penousal Machado
*Centre for Informatics and Systems of the University of Coimbra, Department of Informatics Engineering,
Pólo II - Pinhal de Marrocos, 3030-290 Coimbra, Portugal*

Keywords: Automatic Identification System, Data Visualization, Data Processing, Magnified Fish-Eye Lens.

Abstract: Automatic Identification System data has been used in several studies with different directions like traffic forecasting, pollution control or anomalous behavior detection in vessels trajectories. Considering this last subject, the intersection between vessels is often related with abnormal behaviors, but this topic has not been exploited yet. In this paper an approach to assist the domain experts in the task of analyzing these intersections is introduced, based on data processing and visualization. The work was experimented with a proprietary dataset that covers the Portuguese maritime zone, containing an average of 6460 intersections by day. The results show that several intersections were only noticeable with the visualization strategies here proposed.

1 INTRODUCTION

The Automatic Identification System (AIS) is an international standard for communication between vessels and terrestrial stations developed to improve maritime safety (Tetreault, 2005). AIS data contains all the necessary information for mapping the trajectories followed by each vessel and the general maritime traffic of any sea, and for that reason it has been used in several studies. The majority of these studies are focused particularly in traffic analysis and forecasting (Sang et al., 2016), pollution control (Busler et al., 2015), fusion of different maritime data sources (Xu et al., 2015) or identification of vessels' anomalous behaviors (Handayani et al., 2013; Soleimani et al., 2015). Regarding this last topic, there are a set of common abnormal activities involving two vessels that were identified by the domain experts (e.g. navy operators), such as two vessels sailing very close to each other, which could be an indicator that an illegal trade is happening, and two vessels crossing trajectories, especially if one of them goes from the coast to the intersection zone and comes back after a short period of time, which could be an indicator that this vessel went to the zone to pick up some illegal goods left by the other one. These activities are often related to abnormal intersections between them. Published works in the data visualization field have only been focused in new representations of the traffic situation from specific areas of interest (Willems et al., 2009; Gao and Shiotani, 2013; Chen et al., 2016), with minor or no emphasis on any type of anomalous behav-

iors, including intersections. This work proposes a new approach, based on data processing and visualization, to assist the detection of anomalous behaviors by domain experts, with a particular interest on intersections. This approach solves the following problems from the visualization perspective:

- To process the raw AIS data and extract the intersections from it, a set of data processing tasks are introduced;
- To detect and unveil the intersections within the visual clutter created by all the trajectories, a visual search strategy based on a magnified fish-eye lens is proposed;
- To properly analyze individual intersections by displaying the direction and the speed of the vessels, an animated strategy is introduced that displays the trajectories of the vessels over time;
- To decide which areas of the sea have a higher probability of containing anomalous intersections, a visual selection strategy based on high density areas associated with an abnormality level is introduced.

The approach was experimented with a proprietary dataset that contains data from the Portuguese maritime zone, collected between February 22 and March 12 of 2012. An average of 6460 intersections per day were detected, and the majority are only visible with the proposed visualization strategies. Two case studies are presented as a proof of concept.

The remainder of the paper is organized in the fol-

lowing way: Section 2 presents recent related works that exploit AIS data with visual strategies, Section 3 introduces the proposed approach for the intersections analysis, Section 4 presents a proof of concept with real data and describes the dataset, and Section 5 presents the conclusions and future directions.

2 RELATED WORK

Regarding AIS data visualization, most works are focused on visual strategies to display the traffic patterns, where the trend is to explore density-based visualizations. Chen et al. (Chen et al., 2016) introduced the concept of summary visualization where relevant patterns are visualized through density heat maps that highlight the high-speed and slow-down areas. Willems et al. (Willems et al., 2009) proposed a new kernel density method based on the speed of the vessels that is able to measure the contribution of each vessel in each point of the map. Jiakai et al. (Jiakai et al., 2012) introduced a new data visualization model that divides the region of interest into a grid and calculates an index of the maritime traffic situation for each cell. Gao and Shiotani (Gao and Shiotani, 2013) introduced the usage of 3D visualizations to analyze specific vessels and provide a trustful representation of their environment. Fiorini et al. (Fiorini et al., 2016) proposed a pipeline of actions to go from raw AIS data to a proper visualization of the vessels routes, using only open-source tools, being the final result an interactive web-like geographical visualization. Riveiro and Falkman (Riveiro and Falkman, 2009) introduced an interactive visual analytics model that is able to present the density probability of each combination of several AIS kinematic values.

As stated before, the works described are only focused on presenting the traffic situation of specific areas of interest, through different visual strategies that are often density-based and interactive. In general, minor or no emphasis is given to anomalous behaviors, being this a direction yet to be explored. The approach proposed on this work exploits AIS intersections as anomalies, which consists of a novelty point.

3 PROPOSED APPROACH

The proposed approach for intersections analysis is composed by the extraction tasks and three distinct visualization strategies to address the problems described in section 1. This section describes with detail each of these components.

In order to display the AIS positions several decisions must be made regarding the usage of the visual variables. These decisions are common to the three strategies proposed in this work, and are based on the visual semiology concepts proposed by Jacques Bertin (Bertin, 1983). AIS positions are represented by the cartesian coordinate system, which means that a map projection needs to be applied to the original geographic coordinates (latitude and longitude) of each AIS position. In this work the Spherical Mercator projection is used, mainly because the more important interactive maps platforms, like Google Maps and OpenStreetMaps, also use it. Regarding the visual marks used to represent the AIS positions and intersections, it was decided to represent each position through a circle with a radius of one pixel and each intersection with the same shape but with a radius of five pixels. The intersections are displayed in solid black and each type of vessel has a different color used to paint its positions, meaning that this visual variable is being used for association purposes.

3.1 Intersections Extraction

Before applying any visual method, the AIS raw data must be processed in order to extract the intersections. A first necessary task is to remove the duplicated positions of each vessel. This is an important step because repeated AIS positions will lead to the detection of multiple intersections that are actually the same. This work proposes an approach that isolates the positions of each vessel and detects the ones that are within a minimum time and distance gaps, being these ones labeled as repeated. The time gap is calculated by the absolute difference between the time-stamps of both positions, which are in the UNIX Epoch time format. To calculate the distance between these positions the Haversine formula is used since it considers the curvature of Earth. This algorithm requires as parameters the minimum time and distance gaps. The used values are 15 seconds and one meter and they were obtained empirically. The second and most important task is to detect and extract each intersection between different vessels. For this purpose a new algorithm was introduced that detects an intersection when two positions of different vessels have time and distance gaps below the minimum thresholds passed as parameters. Both gaps are calculated using the same methods from the previous task that removes the duplicated positions. The used values for these parameters are 30 minutes and one kilometer respectively, and they were also obtained empirically. This algorithm does not take into account the direction of the intersection, considering A to B and B to A as different, when they are actually

the same. The algorithm could deal with this issue but that would have impact on its performance and, for that reason, the issue is fixed in a third task that iterates over the intersections, transforms them into sets and calculates a hash for each one. Duplicated hashes are then removed.

3.2 Unveil the Intersections

With all the AIS positions displayed in the same screen a lot of visual clutter may exist. As a consequence, it can become difficult to detect the intersections and even more difficult to analyze each one individually. Therefore, a first necessary step is to create the means for the users to efficiently search and focus on specific intersections. In this work the fish-eye lens (Bettonvil, 2005; Altera, 2008) is used for this purpose. This type of lens applies a convex effect to the image, creating the illusion that it has the shape of a sphere, an effect commonly called barrel distortion. With this effect the center of the image becomes the focus, while the boundaries become gradually distorted. Consequently, the center of the image becomes more zoomed, with the cost of losing some resolution. When combining this type of lens with the movement of the mouse, the users can focus on specific AIS positions and intersections, surpassing the visual clutter issue. Different distortions with specific characteristics can be applied with a fish-eye lens through different mapping functions. The most popular ones are the equidistant, equisolid, orthographic and stereographic (Bettonvil, 2005). The used function in this approach is the orthographic mapping and it was chosen empirically. The conclusion was that this mapping is the one that better distorts the boundaries of the image through a more exaggerated curvature, which gives more focus and zoom to the center. To apply the fish-eye effect two parameters are required: the focal length f_l and the width radius of the lens r_x . Both parameters are correlated and their values can be obtained empirically. Figure 1 shows an example of the fish-eye lens applied with different configurations. On the left an image is displayed with the fish-eye effect using $f_l = 4$ and $r_x = 5$, and on the right the same projection is used but with $f_l = 2$. In this last case, with an increased focal length the zoom was much higher and the pixel interpolation method - which is part of the fish-eye projection - was unable to fill in all the missing gaps, creating the “black pixels” visible on the image. In this work the fish-eye parameters used are $f_l = 3$ and $r_x = 5$, and the effect is only applied to a specific area of interest, which is the area of the map that the user wants to analyze. This area is defined by the mouse position $(mouse_x, mouse_y)$ and



Figure 1: On the left an image displayed with the fish-eye effect applied using $f_l = 4$ and $r_x = 5$, and on the right the same projection but with $f_l = 2$.

by a radius $mouse_r$, that will create a circle around it. An example of this behavior is presented on Figure 2, with the original area displayed on the left and the same area with the fish-eye effect on the right.

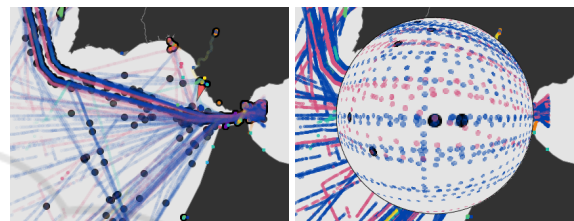


Figure 2: On the left the original area in analysis. On the right the same area with the fish-eye effect applied and the intersections identified.

The application of the fish-eye lens gives the user a way to focus and zoom on a specific area, but the level of magnification may not be enough for an efficient analysis. Increasing the zoom only by defining an higher focal length has growth limitations and will lead to the problem presented on the right image of Figure 1. Therefore, this work combines the fish-eye effect with levels of magnification. The key concept is to render the area of the map in analysis n times, where each time the level of zoom is increased by a scalar $zoom_g$. The zoom of the geographical positions is handled by the majority of the map projections available (including the Spherical Mercator) through a scalar that indicates the magnification to be applied. The maximum number of levels can be predefined or it can be adjusted while the zoom increases, with this last strategy having a performance cost. Assuming that $zoom_c$ is the initial zoom of the area that corresponds to the level $n = 0$, the zoom of each n level is calculated using the formula $zoom_l = zoom_c + (n * zoom_g)$. An important aspect of this method is that the magnification effect needs to be applied to the center of the area in analysis, otherwise it would start to change. To ensure this aspect the cartesian coordinates of each position in each level need to be shifted according to a point of reference from the base level ($n = 0$). This point of reference (x_{rb}, y_{rb}) is the AIS position that has the

minimum euclidean distance between the fixed mouse position $(mouse_x, mouse_y)$ and itself. Considering a point (x_p, y_p) on any given level and the point of reference (x_{rl}, y_{rl}) on the same level, the shift formulas are $x_{new} = (x_p - x_{rl} + (x_{rb} - mouse_x) + mouse_r)$ and $y_{new} = (y_p - y_{rl} + (y_{rb} - mouse_y) + mouse_r)$. These equations also have an adjustment between the point of reference in the base level and the mouse position because this point may not be exactly in the center of the area. To navigate between the levels of magnification the user will first fix the area in analysis through a mouse click and, after that, two controls to change the zoom will appear. Each time the zoom level is updated the fish-eye effect is reapplied. This behavior is presented on Figure 3, displaying the desired effect on the left with the default magnification and the same effect on the right with the third level of zoom. When

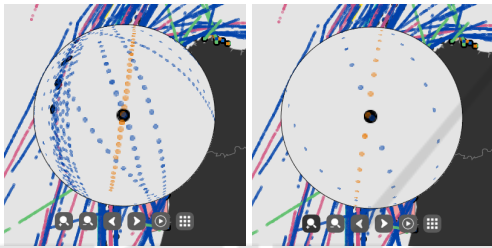


Figure 3: On the left the fish-eye effect with the default magnification. On the right the same effect but with the third level of zoom.

the area in analysis is fixed the intersections inside it are presented individually on a detail lens located on the top-right corner of the screen. This lens has the same level of zoom used on the fish-eye lens and allows the user to analyze each intersection individually without the visual clutter, as Figure 4 shows. The user can change intersections using two controls displayed next to the zoom ones (see Figure 3). When the trajec-

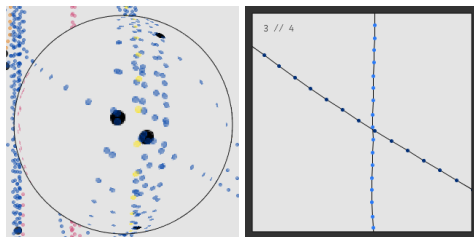


Figure 4: On the left are all the intersections visible through the fish-eye lens. On the right a specific intersection is isolated through the detail lens.

jectories displayed on the detail lens are from two vessels of the same type, the collision of colors can make the identification of the positions from each vessel a difficult task. To fix this issue a lighter and darker color were created for each type of vessel based on

the original palette. These colors are then used when the above scenario happens.

3.3 Individual Intersections Analysis

Visualizing the vessels trajectories of an intersection with a static approach has several limitations regarding the amount of features that can be displayed. With the existing visual variables only the positions of the vessel and its type can be presented. This means that two very important features for behavior analysis are ignored: the speed and the direction. To present these two features this work uses the motion variable, combined with the position and the orientation, through an animation approach that allows the visualization of the vessels moving over time. For the animation to be performed the period in analysis is divided into 15 minutes frames. This interval was used because it includes more than one position by vessel (often two to four positions), which allows a better understanding of the trajectories evolution in terms of direction. Each frame contains the vessels positions from its time interval and the ones from the previous frames, and it is displayed a quarter of a second after the previous one, creating the desired motion effect. Each vessel position is drawn through a circle with a radius of seven pixels. The positions from the current time interval are drawn with an opacity of 100% but the ones that are from previous frames are drawn black with an opacity of only 10% (this value was obtained empirically). This creates a trace effect that allows the perception of how the vessels are moving over time without losing track of their position in the current frame.

The vessels new positions and directions are automatically displayed through the animation as a consequence of the motion effect. The points added in each frame are enough to understand the direction of a vessel because these new points will change the orientation of the trajectory. However, the speed attribute requires further efforts to be visible. An approach was developed where the speed is represented by the accumulative opacity of the vessels trace over time. Assuming that a vessel reports its positions in a fixed period of time (for instance, each five minutes), if this vessel is moving slowly the reported positions will be very close to each other. However, if the vessel is moving fast these positions will be far from each other. When all the positions are drawn at the same time on the trace of the vessel, the ones that are overlaid will generate a higher opacity because their individual colors are blended. This means that the areas of the trajectories where the transparency of the trace is lower are the ones where the vessels are

moving slower, because more points were overlaid for this effect to happen. On the contrary, a trace with a higher transparency corresponds to a vessel moving faster. As stated before, this speed visualization approach only works if the time-span between each position of a vessel is fixed, which is a problem because the AIS communication periods are not consistent. To fix this issue a cubic spline interpolation is applied to every trajectory to generate the missing positions. As stated in the literature (Zhang et al., 2017; Sang et al., 2012), this type of interpolation is the one that adjusts better to the reconstruction of AIS trajectories, offering just some limitations in the presence of very tight curves. This interpolation creates a piecewise function, which means that it defines several small sub-intervals through the domain of x , and has an individual polynomial of degree three for each one. This aspect is important to make the final function more smooth and better suitable for curves. The interpolation is made individually for the latitude and the longitude, being these variables the output y of the generated functions and the timestamp in seconds the input x . The polynomial coefficients of both functions are calculated with all the AIS positions of the respective vessel. Each of these positions is then compared with the one immediately after and, if the time gap between them is over five minutes, new positions are generated through the interpolated functions, with intervals of also five minutes until the gap is filled. This five minutes period was defined empirically. Figure 5 shows an example of a frame from an animation with four vessels sailing at different speeds. It is visible that the tanker vessel (the pink one) in the middle is sailing at a low speed, maintaining a route in a very small area, while the other two tankers sailed faster. The cargo vessel (the dark blue one) started slow but increased the speed roughly in the middle of the trajectory.



Figure 5: An example of a frame from an animation with vessels sailing at different speeds.

3.4 Areas with Anomalous Intersections

The visual search mechanism already described is important to identify and isolate intersections for individual analysis, but when a big quantity of intersections exist within the visible data it may be difficult

to decide where to start the search. With this issue in mind, an approach to identify areas with a higher probability of having anomalous intersections is proposed in this work. The approach can be described in the following steps:

1. Identify the areas, for each day, where the quantity of intersections is higher;
2. Analyze if those areas are constant over the days;
3. Define more frequent areas as less probable of having abnormal behaviors;
4. Visualize the areas and the abnormality levels.

Regarding the first step, areas with a higher quantity of intersections can be seen as clusters with a higher density. Therefore, a density-based clustering strategy was used to extract these areas from the data. Density Based Spatial Clustering of Applications with Noise (DBSCAN) has been used extensively with AIS data and had shown good results (Pallotta et al., 2013; Gonzalez et al., 2014), which made it the most obvious choice for the algorithm to be used. However, this algorithm requires the minimum number of points by clusters ($MinPts$) and the distance between each point and its neighbors (ϵ), and this last one is not easy to estimate because there are zones of the map where the distance between the vessels positions is supposed to be lower (e.g. near the ports) and zones where it is supposed to be higher (e.g. high sea corridors). For this reason the Hierarchical Density Based Spatial Clustering of Applications with Noise (HDBSCAN) was also considered, because it uses an approach where the ϵ value is not required as a parameter and the clusters can have different densities. Both algorithms were experimented with different configurations of the parameters to allow a more effective choice of clusters. Regarding the values of $MinPts$, it was observed by visual analysis that, with the exception of ports, there were no considerable areas with more than 100 intersections. Therefore, this value was used as a maximum and the $MinPts$ was experimented with four values: 25, 50, 75 and 100. Regarding the values of ϵ for the DBSCAN, a maximum of 750 meters was defined and the parameter was experimented with three values: 250, 500 and 750 meters. Notice that the algorithms were applied individually for the AIS data of each day. To choose the better algorithm and configuration the silhouette coefficient was applied to the retrieved clusters, using an euclidean distance for the calculations. The average coefficient results and standard deviations are presented on Table 1 for the best four configurations of both algorithms. The results show that the HDBSCAN with $MinPts = 75$ was the configuration with an higher silhouette coefficient average

while maintaining an acceptable standard deviation. Therefore, it was chosen for the clusters extraction.

Table 1: Silhouette results for HDBSCAN and DBSCAN.

Algorithm	MinPts	ϵ	Avg.	Std.
HDBSCAN	75	NA	0.525	0.084
HDBSCAN	100	NA	0.507	0.081
DBSCAN	25	750	0.499	0.070
DBSCAN	75	750	0.473	0.077

Regarding the second step, the key idea was to associate a frequency to each cluster of each day. To calculate this frequency (F_c) the formula on Equation 1 was proposed.

$$F_c = \frac{\text{Number of days where the cluster exists}}{\text{Total number of days}} \quad (1)$$

Considering the necessary parameters for the formula above, the total number of days with AIS data is a known value but the number of days where each cluster exists needs to be calculated. For this purpose a new algorithm was developed that receives a cluster from a day, the clusters of the remaining days and an overlap threshold (between zero and one). The key idea is to evaluate if the given cluster exists on other days by calculating the area of intersection between it and each of the remaining clusters. This area is then converted to a percentage by dividing it with the area of the given cluster, and if this percentage is greater than the overlap threshold it is considered that the cluster exists on the selected day. The overlap threshold is important in this analysis because it is highly unlikely that two clusters have the exact same shape, which would be necessary for a degree of 100% of overlap. Moreover, the goal is to identify if an area that has a high density in one day also has it in other days, and for that reason a total overlap is not required since the same area may be within a bigger or smaller cluster on others days. For these reasons, the value of this threshold was defined as 50%. Notice that this algorithm could use the overlap of each individual point from the clusters for the calculations, but the required time for the algorithm to compute would be unfeasible. Therefore, the area from the clusters was considered to calculate the overlap, but this is not an immediate operation. In this approach the area is obtained from the convex hulls of the clusters points, which are extracted using the Graham's Scan algorithm (Graham, 1972). The shape of the convex hull adapts well to the clusters, because it considers all the boundaries and is able to represent them without restrictions (being an irregular polygon, it can assume any convex shape). Considering that the coordinates from the vertices are known, the formula presented on

Equation 2 can be used to calculate the area. Notice that the coordinates must be applied in counterclockwise order around the polygon, using the first point also as the last one.

$$A_{cp} = \frac{1}{2} \sum_{k=0}^{n-1} (x_k * y_{k+1} - y_k * x_{k+1}) \quad (2)$$

With the frequency of each cluster calculated, the third step was addressed by associating less common clusters as more likely to include abnormal behaviors. This concept has been used in other studies and relies on the fact that an area where a higher density of intersections is often found should be considered less probable of being abnormal when compared to one where this higher density happens as an exception. Therefore, the level of abnormality of each cluster was calculated based on the frequency using the formula on Equation 3.

$$AL_c = 1 - F_c \quad (3)$$

Finally, addressing the fourth step, to visualize these clusters the convex hulls are drawn on the platform and the visual variable color was used for the representation of the abnormality levels. These levels were discretized into four intervals, namely $[0, 0.25[$, $[0.25, 0.50[$, $[0.50, 0.75[$ and $[0.75, 1]$. A gradient of the color red was created with four levels, each one for a specific interval, where the first level (light red) is the lowest and the fourth level (dark red) is the highest. The convex hull drawn for each cluster is filled with the color that matches its interval of abnormality. Figure 6 shows an example with two areas drawn on the platform. The one from the left has a lower level of abnormality compared to the one on the right.



Figure 6: An example with two abnormal areas drawn on the platform.

4 PROOF OF CONCEPT

The proposed approach was implemented in Java with Processing 3 and tested with real data. An usage example of the implementation is presented in the following video: <https://vimeo.com/304586547>. The used proprietary dataset has AIS data from the Portuguese maritime zone collected between February 22 and March 12 of 2012. It contains positions for

the nine types of vessels available but with very unbalanced quantities for each type, being these the predominant three: cargos with 52%, tankers with 21% and special crafts with 8%. Analyzing the trajectories of the vessels, the following statistics can also be obtained: the dataset contains a total of 9394 trajectories, the average duration of a trajectory is 1.5 days and the average number of trajectories by day is 1085.

Considering the 20 days of data available, each day has an average of 6460 intersections. Figure 7 displays several AIS trajectories from vessels that sailed through the main corridor of the Portuguese maritime area on February 22 of 2012. These maritime corridors are specific areas of the sea where the vessels are supposed to sail, and the traffic density on them is usually very high. The selected day has 4838

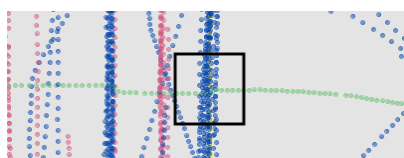


Figure 7: Visualization of several AIS trajectories.

intersections in a total of 86652 positions, which represents a ratio of 5.6%. Apparently the area marked by the black square contains only cargo vessels (the dark blue ones) and a fishing vessel (the green one). Moreover, it appears that the fishing vessel may eventually intersect with several cargos. However, when the intersections are activated and the fish-eye lens is applied on the black square area with at least one level of zoom, an unexpected intersection is revealed. Figure 8 shows this intersection on the fish-eye lens (left image) and on the detail lens (right image). The

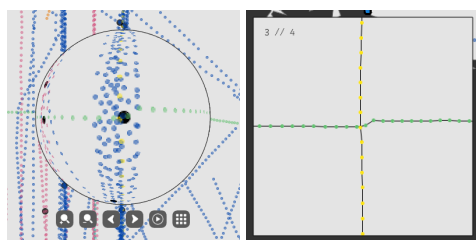


Figure 8: Individual analysis of the intersection. On the left the magnified fish-eye lens is applied. On the right the intersection is isolated through the detail lens.

intersection between the fishing vessel and the passengers vessel (the yellow one) was hidden in the visual clutter created by the trajectories of the remaining ones. Without the usage of the magnified fish-eye lens it would be very difficult to detect and analyze this intersection.

Fishing vessels can be particularly hard to analyze considering that their trajectories are very irregular

when comparing, for example, with cargos or tankers. Figure 9 (left image) displays AIS trajectories from March 10 of 2012. Notice that the cargos and tankers were removed from the screen. The area marked by

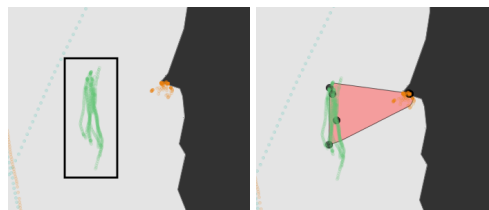


Figure 9: On the left the visualization of the AIS fishing trajectories. On the right the intersections and the high density area of the same trajectories.

the black square on the Figure 9 appears to contain a trajectory from a fishing vessel. However, when the intersections are displayed, the screen shows that there are more than one trajectory from fishing vessels in that area and, more importantly, they intersect in several points. Moreover, the area is considered to have a high density of intersections and the red color indicates that the level of abnormality is three out of four. Figure 9 (right image) shows these intersections and the high density area. When the fish-eye lens is applied on the area the intersections are isolated through the detail lens. Figure 10 shows all intersections on the fish-eye lens (left image) and only the first intersection on the detail lens (right image). Notice that, being the two vessels from the same type, each one is painted with a light or dark green. The an-

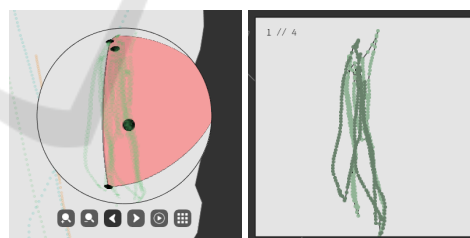


Figure 10: Detection and isolation of the first intersection. On the left the magnified fish-eye lens is applied. On the right the first intersection is isolated through the detail lens.

imation of trajectories was applied to the intersection and, as Figure 11 shows, one of the vessels is always following the other. This pattern could be an important aspect to confirm or discard the behavior as suspicious. The speed of the vessels is more or less constant with the exception of some turning points where it decreases.

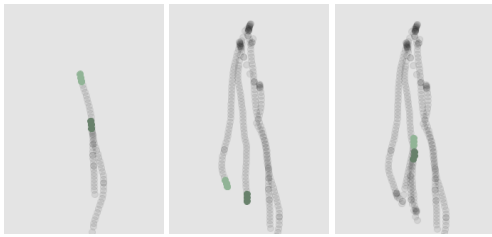


Figure 11: Three frames of the animation from the isolated intersection.

5 CONCLUSIONS

This paper proposes the first approach that is focused on analyzing intersections between vessels through data processing and interactive visualization strategies. The approach consists of several data processing tasks that extract the intersections from the raw AIS data, a visual search strategy based on a magnified fish-eye lens, an animation strategy that allows an individual analysis of the trajectories and a visual selection method based on high density areas and their abnormality levels. The experiments showed that these new strategies help on the detection and analysis of intersections that otherwise would be hidden in the visual clutter. In the future an aspect to explore is the evaluation of the usability and efficiency of the proposed strategies with real users, particularly with domain experts, in order to understand if they have difficulties during the process. Another direction to explore is to obtain more AIS datasets, which will allow new experiments in other contexts.

REFERENCES

- Altera (2008). A flexible architecture for fisheye correction in automotive rear-view cameras. Technical report, Altera Corporation.
- Bertin, J. (1983). *Semiology of Graphics: Diagrams, Networks, Maps*. University of Wisconsin Press.
- Bettonvil, F. (2005). Fisheye lenses. *WGN, Journal of the International Meteor Organization*, 33:9–14.
- Busler, J., Wehn, H., and Woodhouse, L. (2015). Tracking vessels to illegal pollutant discharges using multi-source vessel information. *The International Archives of Photogrammetry, Remote Sensing and Spatial Information Sciences*, 40(7):927.
- Chen, C., Wu, Q., Zhou, Y., and Mao, Z. (2016). Information visualization of ais data. In *Logistics, Informatics and Service Sciences (LISS), 2016 International Conference on*, pages 1–8.
- Fiorini, M., Capata, A., and Bloisi, D. D. (2016). Ais data visualization for maritime spatial planning (msp). *International Journal of e-Navigation and Maritime Economy*, 5:45–60.
- Gao, X. and Shiotani, S. (2013). An effective presentation of navigation information for prevention of maritime disaster using ais and 3d-gis. In *Oceans-San Diego, 2013*, pages 1–6.
- Gonzalez, J., Battistello, G., Schmiegelt, P., and Biermann, J. (2014). Semi-automatic extraction of ship lanes and movement corridors from ais data. In *Geoscience and Remote Sensing Symposium (IGARSS), 2014 IEEE International*, pages 1847–1850.
- Graham, R. L. (1972). An efficient algorithm for determining the convex hull of a finite planar set. *Information processing letters*, 1(4):132–133.
- Handayani, D. O. D., Sediono, W., and Shah, A. (2013). Anomaly detection in vessel tracking using support vector machines (svms). In *Advanced Computer Science Applications and Technologies (ACSAT), 2013 International Conference on*, pages 213–217.
- Jiacai, P., Qingshan, J., Jinxing, H., and Zheping, S. (2012). An ais data visualization model for assessing maritime traffic situation and its applications. *Procedia Engineering*, 29:365–369.
- Pallotta, G., Vespe, M., and Bryan, K. (2013). Vessel pattern knowledge discovery from ais data: A framework for anomaly detection and route prediction. *Entropy*, 15(6):2218–2245.
- Riveiro, M. and Falkman, G. (2009). Interactive visualization of normal behavioral models and expert rules for maritime anomaly detection. In *Computer Graphics, Imaging and Visualization, 2009. CGIV'09. Sixth International Conference on*, pages 459–466.
- Sang, L.-Z., Yan, X.-P., Mao, Z., and Ma, F. (2012). Restoring method of vessel track based on ais information. In *Distributed Computing and Applications to Business, Engineering & Science (DCABES), 2012 11th International Symposium on*, pages 336–340.
- Sang, L.-z., Yan, X.-p., Wall, A., Wang, J., and Mao, Z. (2016). Cpa calculation method based on ais position prediction. *The Journal of Navigation*, 69(6):1409–1426.
- Soleimani, B. H., De Souza, E. N., Hilliard, C., and Matwin, S. (2015). Anomaly detection in maritime data based on geometrical analysis of trajectories. In *Information Fusion (Fusion), 2015 18th International Conference on*, pages 1100–1105.
- Tetreault, B. J. (2005). Use of the automatic identification system (ais) for maritime domain awareness (mda). In *OCEANS, 2005. Proceedings of MTS/IEEE*, pages 1590–1594.
- Willems, N., Van De Wetering, H., and Van Wijk, J. J. (2009). Visualization of vessel movements. In *Computer Graphics Forum*, volume 28, pages 959–966.
- Xu, W., Zhong, D., Wu, S., and Ni, H. (2015). A track fusion method of a vessel. In *Sixth International Conference on Electronics and Information Engineering*, volume 9794, page 97941E.
- Zhang, D., Li, J., Wu, Q., Liu, X., Chu, X., and He, W. (2017). Enhance the ais data availability by screening and interpolation. In *Transportation Information and Safety (ICTIS), 2017 4th International Conference on*, pages 981–986.